Vol 11 No 6, June 2002
1009-1963/2002/11(06)/0613-06

Chinese Physics

© 2002 Chin. Phys. Soc.
and IOP Publishing Ltd

Spectroscopic properties of Nd-doped phosphate glass with a high emission cross section*

Mao Yan-Li(毛艳丽)[a)b)], Sun Zhen-Rong(孙真荣)[c)], Jiang Xiu-Li(蒋秀丽)[c)], Deng Pei-Zhen(邓佩珍)[a)], and Gan Fu-Xi(干福熹)[a)]

[a)] *Shanghai Institute of Optics and Fine Mechanics, Chinese Academy of Sciences, Shanghai* 201800, *China*
[b)] *Department of Physics, Henan University, Kaifeng* 475001, *China*
[c)] *Department of Physics, East China Normal University, Shanghai* 201800, *China*

(Received 20 December 2001; revised manuscript received 26 January 2002)

Neodymium doped phosphate glasses have been prepared by the semi-continuous melting technique. Their absorption and emission spectra have been recorded at room temperature. The Judd–Ofelt theory has been applied to evaluate the stimulated emission cross sections of $^4F_{3/2}\rightarrow{}^4I_{11/2}$ transition for Nd^{3+}. The higher stimulated emission cross section, $4.0\times10^{-20}cm^2$, is obtained. The fluorescence decays of the $^4F_{3/2}\rightarrow{}^4I_{11/2}$ transition of Nd^{3+} are measured for the samples doped (0.7–10) wt% of Nd_2O_3 at room temperature. The concentration quenching of Nd-doped phosphate glass is mainly attributed to cross-relaxation and energy migration. The site-dependent properties of fluorescence spectra and the fluorescence lifetime of the Nd^{3+}-doped phosphate glass (with 2.2wt% Nd_2O_3) are studied using laser-induced fluorescence line narrowing techniques, and the site-to-site variations of optical properties are observed at low temperature.

Keywords: Nd^{3+} ions, phosphate glass, emission cross section, fluorescence line narrowing
PACC: 7845, 7855

1. Introduction

Neodymium-doped phosphate glasses are the preferential material for use in high-energy and high-peak-power laser systems.[1−3] There are three important reasons. Firstly, energy can be efficiently stored and extracted from these glasses.[4,5] Secondly, high-energy storage densities can be achieved.[2,4] Thirdly, the glass can be manufactured in metre-scale sizes with high optical homogeneity and low Pt-inclusion concentrations.[6] One of the particularly significant properties of lasing materials for high-power lasers is the gain coefficient, which correlates to the emission cross section. Therefore, although Nd-doped phosphate glass has been investigated during the last three decades, there is still interest in developing high emission cross-section Nd-doped phosphate glass.

It is known that knowledge of the spectroscopic properties of Nd^{3+} ions is of fundamental importance for laser action.[7,8] These properties include spectral absorbance, peak wavelengths and linewidths, branching ratios, emission cross section, fluorescence lifetime, quantum efficiencies, and fluorescence quenching processes. The relationship between these parameters and the nature of the glass host is also of particular interest for developing new laser materials.

The spectroscopic and laser properties of rare-earth ions are strongly affected by the local structure at the rare-earth sites and the distribution of the doped ions in the glass matrix. For a glass laser, the effects of site-to-site variations, in the large-signal gain regime, cause hole burning and reduced energy output. Therefore, the knowledge of the distribution of spectroscopic properties for laser ions in glass is important for selecting the optimum host glass and operation conditions.[9,10]

In this paper, we report on a spectroscopic study of Nd^{3+}-doped phosphate glasses with high stimulated emission cross sections. Using Judd–Ofelt (JO) theory, we determined their optical parameters. The fluorescence quenching processes are investigated. The site-dependent effects of emission properties are studied by the fluorescence line narrowing (FLN) technique at low temperature.

2. Experiment

Phosphate glasses were prepared using a semi-continuous melting technique. The compositions ex-

*Project supported by the National Natural Science Foundation of China (Grant No 69988006).
†Corresponding author: Mao Yan-Li E-mail: maoyanli@163.net

amined belong to the P_2O_5–Al_2O_3–BaO–K_2O–Li_2O–Nb_2O_5–La_2O_3 system. The samples investigated are doped with various concentrations of Nd_2O_3. The phosphate glasses were first melted at 1500–1600K in a platinum crucible in air. The melt was then poured on to a stainless-steel plate and cooled to room temperature. Finally, the samples were polished to obtain slides for optical measurements.

Conventional absorption spectra were performed with a Lambda 900 spectrophotometer. The fluorescence spectra were recorded in an infrared Fourier spectrometer (model Nexus 870 FT-IR, nicolet) using a tunable Ti:sapphire laser as the excitation source (tuning range 850–950nm). Lifetime measurements were performed with a tunable dye laser of 10ns pulse width and 0.08cm^{-1} linewidth. The emitting light was detected through a 0.5m monochromator with a photomultiplier. Luminescence was recorded in a 500Hz digital oscilloscope. The low temperatures below 300K were achieved using a continuous-flow liquid helium cryostat with a temperature accuracy of ±1K.

3. Results and discussion

3.1. Absorption properties

The room-temperature absorption spectra are recorded for all samples in the 300–1000nm spectral range. The absorption spectrum of the sample (with 2.2wt% Nd_2O_3) consists of a large number of lines (Fig.1) attributed to transitions occurring within the 4f shell of the Nd^{3+} ion. Data from these spectra can be used to calculated the intensity parameters, the branching ratios and the radiative transition probabilities of fluorescence transitions of $^4F_{3/2} \rightarrow {}^4I_J$ manifolds and so on, according to the JO theory.[11,12]

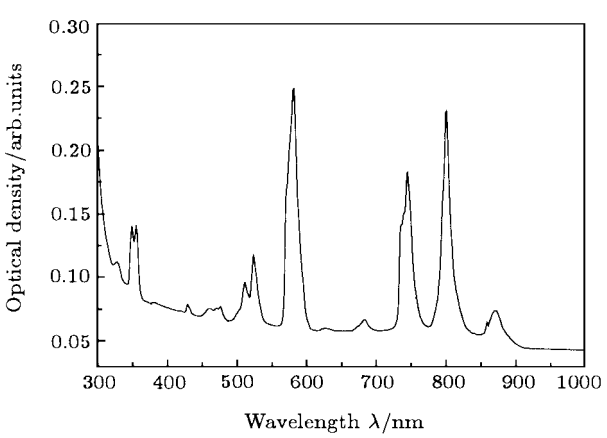


Fig.1. Absorption spectrum of the neodymium-doped phosphate glass (with 2.2wt% Nd_2O_3).

The oscillator strengths of the absorption bands are calculated for the samples, using the expression

$$f = \frac{mc^2}{\pi e^2 N}\frac{2.303}{d}\int \frac{\mathrm{OD}(\lambda)\mathrm{d}\lambda}{\lambda^2}, \qquad (1)$$

where m and e are the electron mass and charge respectively, c is the velocity of light, $\mathrm{OD}(\lambda)$ is the optical density, and d is the sample thickness. The experimental f values have been used to calculate the Ω_t parameters corresponding to the JO theory. Using the theory, the line strength of electric–dipole transitions between J initial $|(S,L)J\rangle$ and terminal $|(S',L')J'\rangle$ manifolds may be written in the form[13]

$$S = \sum_{t=2,4,6} \Omega_t |\langle (S,L)J||U^{(t)}||(S',L')J'\rangle|^2, \qquad (2)$$

where the elements $\langle||U^{(t)}||\rangle$ are the doubly reduced unit tensor operators, and are almost independent of the ion environment. The numerical values of the unit tensor operators of Nd^{3+} have been calculated by Carnall *et al.*[14] The three coefficients Ω_2, Ω_4 and Ω_6 contain implicitly the odd-symmetry crystal-field terms, radial integrals, and perturbation denominators. The oscillator strength of a transition can be written as

$$f = [8\pi^2 m\nu/3h(2J+1)][(n^2+2)^2/9n]S, \qquad (3)$$

where m is the electron mass, ν is the frequency of the transition, J is the total angular momentum of the initial level (J=9/2 in Nd^{3+}), and n is the refractive index. The best set of Ω_t parameters can be determined by a least-squares fitting of the calculated f values given by Eq.(3) to the experimental values. The JO parameters obtained from this fitting are given in Table 1.

The spontaneous emission probabilities between the excited J manifolds of the Nd^{3+} ions in glass can be calculated from the Ω_t parameters. The radiative transition probability from the initial J' manifold $|(S',L')J'\rangle$ to the terminal manifold $|(S,L)J\rangle$ is given by[15]

$$\begin{aligned} &A[(S',L')J';(S,L)J] \\ &= \frac{64\pi^2 e^2}{3h(2J'+1)\lambda^3} n \frac{(n^2+2)^2}{9} \\ &\quad \times \sum_{t=2,4,6} \Omega_t |\langle (S',L')J'||U^{(t)}||(S,L)J\rangle|^2, \end{aligned} \qquad (4)$$

where $(n^2+2)^2/9$ is the local-field correction for the Nd^{3+} ion in the initial J' manifold, n is the refractive index, λ is the wavelength of the transition, and J is

the terminal manifold. The branching ratios can be obtained from the transition probabilities by using[15]

$$\beta[(S'L')J';(S,L)J] = \frac{A[(S',L')J';(S,L)J]}{\sum_{S,L,J} A[(S',L')J';(S,L)J]}. \quad (5)$$

The Ω_t parameters and branching ratios for the fluorescence from the $^4F_{3/2}$ to the ^4I_J states are listed in Table 1.

Table 1. Judd–Ofelt calculation results.

Ω_2	3.9
Ω_4	4.6
Ω_6	5.3
Transition $^4F_{3/2} \rightarrow$	β
$^4I_{9/2}$	0.431
$^4I_{11/2}$	0.478
$^4I1_{3/2}$	0.09

According to Jørgensen and Resifeld,[16] Ω_2 is a measure of the covalence degree related to the established rare-earth ion–ligand bonds. Moreover, the Ω_2 parameter reflects the non-symmetry of the Nd^{3+} local environment; the weaker the Ω_2 value, the more centrosymmetrical the ion site is and the more ionic its chemical bonds with the ligands. The obtained value of Ω_2 in the phosphate glass system, 3.9, indicates that the larger asymmetry is connected with their chain structure compared to other systems.[17]

3.2. Emission properties

The $^4F_{3/2} \rightarrow ^4I_{9/2}$, $^4I_{11/2}$ and $^4I1_{3/2}$ steady-state fluorescence spectra at room temperature is measured for the phosphate glass with 2.2wt% of Nd^{3+} by exciting the sample with an Ar laser (Fig.2). The emission spectrum consists of three large and non-symmetric bands centred near 897, 1054 and 1325nm, and they are inhomogeneously broadened due to site-to-site variation in the local ligand field. Since the emission band is asymmetric, an effective linewidth of the fluorescence intensity I defined by[18]

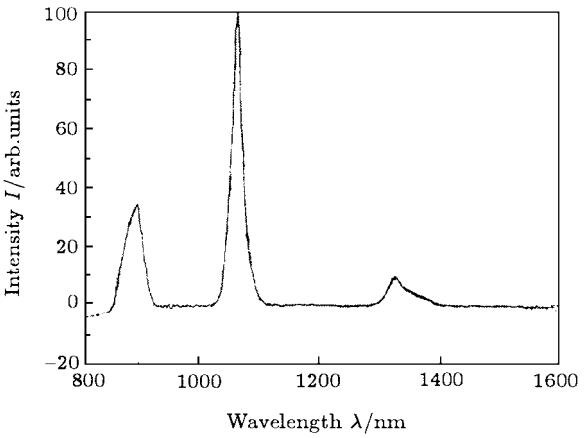


Fig.2. Room-temperature fluorescence spectrum of Nd^{3+} in phosphate glass (with 2.2wt% Nd_2O_3).

$$\Delta\lambda_{\text{eff}} = \int \frac{I(\lambda)\mathrm{d}\lambda}{I_{\max}} \quad (6)$$

is used instead of the full width at half maximum linewidth. $I_{\max}$ is the intensity at the peak fluorescence emission wavelength. The stimulated emission cross section of the $^4F_{3/2} \rightarrow ^4I_{11/2}$ transition can be calculated by the relation[18]

$$\sigma_p(\lambda_p) = \frac{\lambda_p^4}{8\pi c n^2 \Delta\lambda_{\text{eff}}} A[(^4F_{3/2});(^4I_{11/2})], \quad (7)$$

where λ_p is the peak fluorescence wavelength, n is the refractive index, and $\Delta\lambda_{\text{eff}}$ is the effective linewidth of the transition. The stimulated cross section for the $^4F_{3/2} \rightarrow ^4I_{11/2}$ transition is shown in Table 2 together with the effective fluorescence linewidth.

Table 2. Room-temperature emission properties of Nd^{3+}(2.2wt% of Nd_2O_3) in the phosphate glass.

	λ_p/nm	$\Delta\lambda_{\text{eff}}$/nm	$\sigma_p/10^{-20}\text{cm}^2$	n	τ_{exp}/μs
$^4F_{3/2} \rightarrow ^4I_{11/2}$	1054	25	4.0	1.52	330

The $^4F_{3/2} \rightarrow ^4I_{11/2}$ emission cross section in our system is much higher than those obtained in other systems.[17,19,20] The larger cross section is due mainly to the narrower effective emission linewidths. In phosphate glasses, there is a systematic decrease in the effective linewidth with decreasing charge and increasing size of the glass-modifying cations.[21,22] Therefore the introduction of the K_2O modifier has the effect of reducing the emission bandwidth. Furthermore, our glass composition, having the advantage of containing large phosphate proportions (about 60mol% P_2O_5), allows the increase of the absorption and the stim-

ulated emission cross section according to Seeber *et al.*[23] Additionally, the larger Ω_2 value indicates the larger asymmetry in the ligand field of Nd^{3+}, which leads to the larger radiative decay rate.[24] According to the relation(7), the emission cross section σ_p is affected by the radiative decay rate, and the larger radiative decay rate is beneficial to improving the σ_p.

3.3. Luminescence decay

The decays of the $^4F_{3/2} \rightarrow {}^4I_{11/2}$ transition are performed with a narrow band tunable dye laser exciting the sample at the $^4I_{9/2} \rightarrow {}^4G_{5/2}$ absorption band (575nm). The measured fluorescence lifetime at room temperature of the seven samples with different Nd^{3+} concentrations are displayed in Fig.3. As can be observed, the lifetime τ linearly decreases when the Nd^{3+} concentration n increases. The rate of concentration quenching in the phosphate glass is lower than that in silicate glass, because the interactions of Nd–Nd ions are weaker due to the chain structure of phosphate glass. Additionally, the data from the studies[25–28] show that the use of low field strength modifiers, such as K and Ba, reduces the concentration quenching. Both modifiers K and Ba are used in our laser glass compositions, so the concentration quenching effects are small.

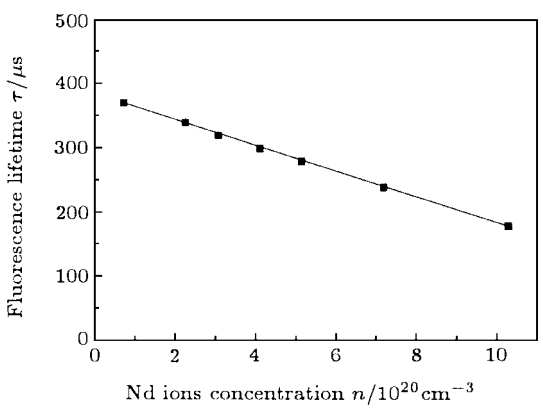


Fig.3. Lifetime of the $^4F_{3/2}$ state as a function of the neodymium ion concentration at room temperature.

In general, at low Nd^{3+} concentrations, emission and multiphonon relaxation dominate the decay of the $^4F_{3/2}$ level. At higher Nd^{3+} concentrations, energy transfer processes take place. Energy transfer processes are cross-relaxation between Nd^{3+} ions and energy migration to hydroxyl group. The multiphonon relaxation rate decreases exponentially as the energy gap between neighbouring energy levels increases. Owing to the high vibration frequencies of the phosphate groups ($1121cm^{-1}$),[29] this process is more probable in phosphate glasses than in the other oxides. However, experience has shown that the multiphonon process contribution to the decay does not exceed 10% in phosphate glasses at room temperature. According to Miyakawa and Dexter,[30] this is due to the relatively large energy gap between the $^4F_{3/2}$ state and the next lower J manifold ($7407cm^{-1}$). The content of quenching OH groups in phosphate glasses is considerably higher than that in fluoride phosphate glasses and silicate glasses due to its hydrophilicity. Therefore, energy transfer from the $^4F_{3/2}$ level to OH groups plays an important role in phosphate glasses, and reduces the $^4F_{3/2}$ state lifetime. In our glasses system, the hydroxyl group absorption is less than $1.0cm^{-1}$ at $3000cm^{-1}$, which will ensure optimum laser performance.[31] In a word, the extinction of the Nd^{3+} luminescence in the phosphate glass is mainly attributed to cross-relaxation and energy transfer processes to the hydroxyl group OH with increasing Nd concentration.

3.4. Site-dependent effects

Taking advantage of the tunability and narrow bandwidth of the Ti:sapphire ring laser as an excitation source for the $^4I_{9/2} \rightarrow {}^4F_{3/2}$ transition, we have obtained the emission spectra of the $^4F_{3/2} \rightarrow {}^4I_{11/2}$ transition at different excitation wavelengths along the $^4I_{9/2} \rightarrow {}^4F_{3/2}$ absorption band of the Nd^{3+}-doped phosphate with 2.2 wt% Nd_2O_3 concentration. Figure 4 shows the steady-state emission spectra obtained at different excitation wavelengths measured at 77K. None of the laser-excited fluorescence spectra shows the extreme line narrowing in spite of the good resolution of our narrow bandwidth Ti:sapphire ring laser. Instead , the linewidths of the $^4F_{3/2} \rightarrow {}^4I_{11/2}$ transition are much broader than the homogeneous widths. This is attributed to a residual inhomogeneous broadening, which occurs for nonresonant fluorescence, because the excitation energy of ions in physically distinct sites may accidentally coincide while the location of other levels remains different.[32] However, the characteristics of site-selection of spectra still shows. As can be observed, the spectrum slightly narrows and redshift occurs as the excitation wavelength increases, and the shape of the emission band changes as excitation wavelength varies.

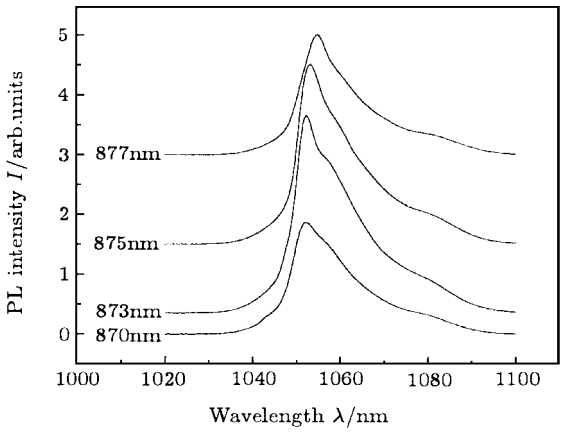


Fig.4. Steady-state emission spectra of the $^4F_{3/2} \rightarrow {}^4I_{11/2}$ transition in phosphate glass with 2.2wt% of Nd_2O_3 for different excitation wavelengths. Measurements were performed at 77K.

The fluorescence decay for the $^4F_{3/2} \rightarrow {}^4I_{11/2}$ emission is also measured as a function of the excitation wavelength along the $^4I_{11/2} \rightarrow {}^4G_{5/2}$ absorption band at 6K using a dye laser. The variations in the fluorescence lifetime τ with excitation wavelength are shown in Fig.5, which displays that longer decay times occur at shorter excitation wavelengths and shorter decay times occur at longer excitation wavelengths.

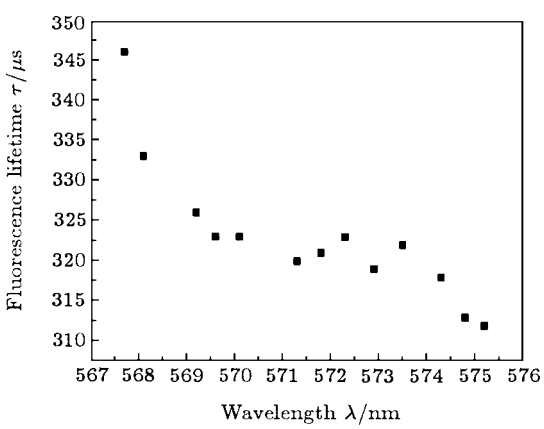


Fig.5. Lifetime τ of the $^4F_{3/2}$ state as a function of excitation wavelength for the phosphate glass with 2.2wt% of Nd_2O_3. Lifetimes were obtained at 6K and collecting the fluorescence at the emission peak of the $^4F_{3/2} \rightarrow {}^4I_{11/2}$ transition.

These results suggest that the Nd^{3+} in phosphate glasses has a different nearest-neighbour coordination. At the shorter wavelength excitations we should observe emissions from Nd^{3+} ions with the larger field strength of ligand D_q, whereas at the longer wavelength excitations emission from smaller field strength of ligand D_q sites becomes dominant. According to non-radiative transition theory,[33] the ions with larger D_q values have a larger energy gap between the excited state and ground state, higher radiative transition probabilities, and so possess shorter emission wavelength, lower non-radiative decay rates and larger fluorescence lifetimes. The ions with smaller D_q values have reverse properties. Therefore, the peaks of emissions wavelengths shift to high energy and the longer lifetime with the excitation energy increases. The distribution of lifetime as a function of excitation energy gives us a picture of the type of local coordination around the Nd ion. However, compared to other Nd^{3+}-doped glasses system,[34] the smaller site-to-site variation in the fluorescence lifetime indicates that the phosphate glass has smaller site-to-site variations in the local field and a comparatively low degree of inhomogeneous broadening. So it has a relatively higher emission cross section.

4. Conclusion

We have studied the spectroscopic properties of the Nd^{3+}-doped phosphate glasses. Using the JO theory, three intensity parameters and stimulated emission cross section between initial $^4F_{3/2}$ and terminal $^4I_{11/2}$ levels of Nd^{3+} were determined. The higher stimulated emission cross section, $4.0\times10^{-20}cm^2$, was obtained, which is mainly attributed to introduction of the K_2O modifier. The fluorescence times of the $^4F_{3/2}$ state of the Nd^{3+}-doped phosphate glasses with different Nd concentrations were measured. Quenching of the Nd^{3+} fluorescence is present as the concentration rises. The influence of the local coordination ions on the optical properties of Nd^{3+} in phosphate glass investigated by fluorescence line-narrowing spectroscopy has shown that Nd^{3+} ions in different sites possess different emission wavelengths and fluorescence lifetimes. Longer lifetimes and shorter emission wavelengths correspond to the Nd^{3+} ions surrounded by higher field strength of ligand.

References

[1] Hunt J T and Speck D R 1989 *Opt. Eng.* **28** 461
[2] Van Womterghem B M *et al* 1997 *Appl. Opt.* **36** 4932
[3] Murray J 1998 *Proc. SPIE* **3492** 1
[4] Campbell J and Suratwala T 2000 *J. Non-Cryst. Solids* **263/264** 318

[5] Koechmer W 1996 *Solid-State Laser Engineering* (New York: Springer) p 4
[6] Campbell J *et al* 2000 *J. Non-Cryst. Solids* **263/264** 342
[7] Weber M J 1990 *J. Non-Cryst. Solids* **123** 208
[8] Feng Y *et al* 2001 *Acta Phys. Sin.* **50** 335 (in Chinese)
[9] Weber M J 1982 *J. Non-Cryst. Solids* **47** 117
[10] Zhang L 2001 *Chin. Phys.* **10** 58
[11] Judd B R 1962 *Phys. Rev.* **127** 750
[12] Ofelt G S 1962 *J. Chem. Phys.* **37** 511
[13] Krupke W F 1966 *Phys. Rev.* **145** 325
[14] Carnall W T, Fields P R and Rajnak K 1968 *J. Chem. Phys.* **49** 4424
[15] Krupke W F 1974 *IEEE J. Quant. Electron.* **10** 450
[16] Jørgensen C K and Resifeld R 1983 *J. Less-Common. Met.* **93** 107
[17] Ajroud M, Haouari M, Ben Ouada H, Maaref H, Brenier A and Garapon C 2000 *J. Phys.: Condens. Matter* **12** 3181
[18] Jacobs R R and Weber M J 1976 *IEEE J. Quantum Electron.* **12** 102
[19] Mehta V, Aka G, Dawar A L and Mansingh A 1999 *Opt. Mater.* **12** 53
[20] Kumar G A, Biju P R, Venugopal C and Unnikrishnan N V 1997 *J. Non-Cryst. Solids* **221** 47
[21] Deutschbein O K and Pautrat C C 1968 *IEEE J. Quantum Electron.* **4** 48
[22] Brawer S A and Weber M J 1981 *J. Lumin.* **24/25** 115
[23] Seeber W, Ehrt D and Ebendorff-Heidrpriem H 1994 *J. Non-Cryst. Solids* **171** 94
[24] Izumitani T and Toratani Kuroda H 1982 *J. Non-Cryst. Solids* **47** 87
[25] Byun J O, Kim B H, Hong K S, Jung H J, Lee S W, Ryoo K S, Izyneev A A and Kravchenko V B 1994 *Japan. J. Appl. Phys.* **33** 4907
[26] Ebendorff-Heidepreim H, Seeber W and Ehrt D 1995 *J. Non-Cryst. Solids* **183** 191
[27] Lunter S, Dyminkov A, Przhevuskii A and Federov Y 1991 *Proc. SPIE* **1513** 349
[28] Jiang Y, Jiang S and Jiang Y 1989 *J. Non-Cryst. Solids* **112** 286
[29] Haouari M, Ben Ouada H, Maaref H and Legrand A P 1997 *J. Phys.: Condens. Matter* **9** 6711
[30] Miyakawa T and Dexter D L 1970 *Phys. Rev.* B **1** 2916
[31] Marion J E and Weber M J 1991 *Eur. J. Solid State Inorg. Chem.* **28** 271
[32] Weber M J, Paisner J A, Sussman S S, Yen W M, Riseberg L A and Brecher C 1976 *J. Lumin.* **12/13** 729
[33] Auzel F 1978 *Luminescence of Inorganic Solids* (New York: Plenum) p 67
[34] Brecher C, Risberg L A and Weber M J 1978 *Phys. Rev.* B **18** 5799